



Influence of liquid properties of colloidal crystals to thermal stability of colloidal crystals on different substrate surfaces through heterogeneous nucleation

Seiya Watanabe¹ · Jianhua Ren² · Isao Tabata³ · Kazumasa Hirogaki²

Received: 20 November 2023 / Revised: 3 March 2024 / Accepted: 4 March 2024
© The Author(s) 2024

Abstract

The effects of liquid properties, such as pH and conductivity, on the thermal stability of electrostatically interacting colloidal silica crystals generated from heterogeneous nuclei were investigated mainly by measuring relative reflection spectra. The melting behavior of the colloidal crystals was also investigated. The melting points of both negatively and positively charged 3-aminopropyltriethoxysilane (APS)-treated substrates with different surface charges increased or decreased with increasing or decreasing pH. For both substrates, pH 5.5 was the modulation point of the crystal melting, and the melting point increased with increasing pH. For the negatively charged substrate, the melting point increased slowly as the pH decreased from pH 5.5. Meanwhile, the melting point of the APS-treated substrate increased more with decreasing pH from 5.5 than that of the negatively charged substrate. The cationisation of the substrate increased with decreasing pH, resulting in stronger electrostatic interactions with the negatively charged colloidal crystals and enhanced thermal stability. Next, we investigated the size of colloidal crystal grains in sample bottles for different liquid properties, and the results show that at the higher pH, the smaller crystal grains, indicating that pH affects both the substrates and crystals. Moreover, the binding effect of the APS-treated substrate on the crystals became stronger at lower pH, thereby enhancing the thermal stability of the crystals.

Keywords Silica particle · Colloidal crystals · Heat stability · Melting temperature · Structure color · pH

Introduction

A colloid is a mixture wherein a substance as fine as 1 nm to 1 μm is dispersed in a medium, such as a liquid, gas, or solid. Colloidal crystals are formed in a colloidal dispersion wherein solid colloidal particles are dispersed in a liquid, such as water, in stable, regular lattice-like arrays. The arrays selectively reflect light according to Bragg's law and exhibit beautiful color and brilliance when their periodicity is equal to the wavelength of light [1]. The phenomenon is called structural coloration and exhibits the elegant color of peacock

feathers and morpho butterfly wings. Because the structural color is generated from the optical properties exhibited by the microstructure of colloidal crystals, no discoloration or fading occurs if the structure is maintained. Colloidal crystals are expected to be used for sensors and displays as optical materials and for coloring fibers and polymer materials as substitutes for organic dyes. There are two types of colloidal crystals: tightly packed colloidal crystals—wherein particles contact each other and are oriented—and loosely packed colloidal crystals—wherein particles carry an electric charge in water and are regularly arranged without contacting each other by electrostatic repulsion through an electric double layer [2]. The latter are also called electrostatically interacting colloidal crystals, and their crystal structure can be controlled by adding an electric charge to the substrate. Therefore, because of their ability to control structural coloration, they are expected to be applied to structural color sensors and displays. In this study, we focus on electrostatically interacting colloidal crystals. Silica can generate colloidal crystals [3]. Silica particles are negatively charged in water because of the dissociation of silanol groups on their surfaces, and counterions form a

✉ Kazumasa Hirogaki
hirogaki@u-fukui.ac.jp

¹ Graduate School of Engineering, University of Fukui, 3-9-1 Bunkyo, Fukui 910-8507, Japan

² Headquarters for Carbon Neutral Initiatives, University of Fukui, 3-9-1 Bunkyo, Fukui 910-8507, Japan

³ School of Engineering, University of Fukui, 3-9-1 Bunkyo, Fukui 910-8507, Japan

layer of ions. There is a fixed layer adsorbed on the particle surfaces and a diffuse layer that diffuses from the particle surfaces to a certain area [4]. When a dispersion of colloidal particles in water is desalted and the ionic strength is adjusted, the concentration of negative charges fixed on the particle surfaces does not change but the positive charges around the particles decrease, thereby binding the positive charges that drift far from the particles and expanding the electric double layer [5]. At higher pH of colloidal crystals, the number of charges on the particle surface increases and the density of electric double layer increases with increasing counter ions interact with the surface charges of the particle; while at lower pH, the density of the electric double layer decreases. When the particles containing the electric double layer exceed the average interparticle distance, they are fixed in space and only oscillate in motion due to interparticle repulsion, thereby crystallizing *in situ* [6]. When electrostatically interacting colloidal crystals are applied to a material, they form heterogeneous nuclei and grow from the material surface with the densest faces of the crystal lattice oriented. In this process, crystals grow from a dense crystal lattice formed by particles aligned parallel to the surface [6, 7]. When heterogeneous nuclei crystallize, the resulting crystals are aligned with the surface, making them easy to employ for optical properties applicable to structural coloration. Because silica particles are negatively charged in liquid, there have been reports of deposited colloidal crystals forming due to electrostatic interaction between the particles and substrate by imposing a positive charge of opposite sign on the substrate surface [8–10]. However, the electrostatic interaction between the substrate and particles is unknown. We have previously shown that in electrostatically interacting colloidal crystals formed from heterogeneous nuclei, the electrostatic interaction between the substrate and particles controls particle mobility on the substrate and improves the thermal stability of the crystal lattice structure on the substrate [2, 11]. However, more precise control of the melting point difference of colloidal crystals is necessary to realize sensor and display applications based on structural coloration. In this study, we further investigate the thermal stability of colloidal crystals. Based on the lattice structure stability of electrostatically interacting colloidal crystals formed from heterogeneous nuclei, we specifically analyze the effects of liquid properties, such as pH and conductivity, on the thermal stability of colloidal crystals formed on substrates with different charge properties.

Materials and methods

Preparation of colloidal dispersions

A silica colloidal dispersion (KE-W10, purchased from Nippon Shokubai Co., Ltd.) containing 10%–20% silica

particles (amorphous), 80%–90% water, and 0.1%–0.9% ethylene glycol (impurity) was employed. The particle size of silica particles was 110 nm, and the particle size distribution was measured by dynamic scattering. The average pore size was 112.7 nm [12]. Ultrapure water (18.2 M Ω -cm) was added to the silica colloidal dispersion to adjust the concentration to 4.8 vol%. The ultrapure water was obtained from an ultrapure water production unit (Thermo Fisher Scientific). The silica colloidal dispersion (4.8 vol%) was then desalted by dialysis and ion exchange resin addition, and the crystallization conditions [11] were met. Particle concentration in the dispersion, salt concentration, and the number of surface charges on the silica particles—all of which influence crystal growth—satisfy the crystallization conditions [13]. The liquid properties (pH and conductivity) of the colloidal dispersion were then adjusted by adding 0.1-M sodium hydroxide solution (purity \geq 97%, Nakalitesque Corporation). The pH was measured using a tabletop pH and water quality analyzer LAQUA (Horiba, Ltd.), and the conductivity was measured using a tabletop conductivity meter (DS-52, Horiba, Ltd.).

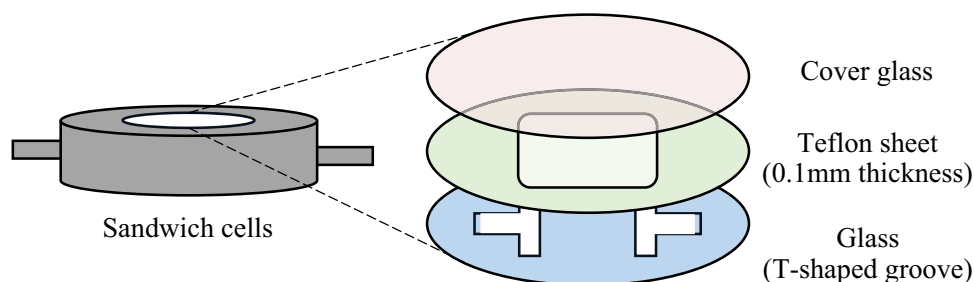
Glass substrate processing

The hydrophilic treatment of glass is described below. Glass (BIOPTech) was ultrasonically cleaned in toluene (Nacalai Tesque Co., Ltd.), acetone (Fujifilm Wako Pure Chemicals) and ultrapure water for 15 min each. The cleaned glass was immersed in sulfuric acid (purity: 95.0%, Nacalai Tesque Co., Ltd.) and allowed to stand for at least 1 day. The glass was then immersed in ultrapure water and allowed to stand for 1 day. The following describes the glass aminosilane treatment. The hydrophilic-treated glass substrates were further treated via the sol–gel method using 3-aminopropyltriethoxysilane (APS) (FUJIFILM Wako Pure Chemicals Corporation) to introduce amino groups. The glass substrates were immersed for 30 s in APS solution (4.5 wt%) that has been stirred for 48 h in a water bath at approximately 27 °C, dried at room temperature, and then heated at 130 °C for 30 min. This cycle was repeated six times to introduce amino groups on the substrates [2, 12].

Glass substrate contact angle measurements

Ultrapure water (5 μ l) was dropped at five locations on the glass substrates, and contact angles were measured via the tangential method using an automatic contact angle meter (Kruss DSA20 (Easy Drop), R-DEC Co.

Fig. 1 Schematic diagram of the Sandwich cells



X-ray photoelectron spectroscopy (XPS) measurements

Elemental analysis of the glass substrates was performed using XPS (JPS-9010MCY, JEOR Ltd.)

Flow and measurement of silica particle dispersion

As shown in Fig. 1, a 0.1-mm-thick polytetrafluoroethylene sheet with rectangular ($14 \times 22 \text{ mm}^2$) holes was sandwiched between a glass substrate with T-shaped grooves (130,119-5NC, BIOPTECH) and a cover glass (40–1313-0319–100, BIOPTECH). The T-shaped groove glass and cover glass were surface treated as described in the glass substrate treatment method. A temperature-variable sandwich cell was constructed by connecting a sandwich cell to a temperature controller (NCB-1200, Tokyo Science Instruments Co). The colloidal dispersion solution meeting the crystallization conditions was passed into the sandwich cell, and the crystals were melted by shear stress and recrystallized after the flow was stopped. A USB-4000 spectrometer (Ocean) was used to measure the relative reflectance of crystals due to inhomogeneous nucleation from the substrate at 0° incidence angle into the cell and 0° detection angle at each temperature [12].

Patterning based on melting point difference

On the left half of one negatively charged substrate, an amino group was introduced by APS, and colloidal crystals were uniformly formed. The sandwich cell was then heated, and the colloidal crystals were photographed using a camera (iPhone 11, GZ-RY980 (JVC)) at 0° incidence and reflection angle for each temperature.

Size of colloidal crystal grains with different liquid properties

For future applications of colloidal crystals, we observed colloidal crystals crystallized in sample bottles using a camera (iPhone 11) to investigate the differences in the perceived size of the crystal grains with respect to differences in liquid properties (pH and conductivity).

Results and discussion

Characteristics of glass substrates

Contact angle measurements showed that the untreated and APS-treated substrate surfaces had contact angles of 40° . The contact angle of the hydrophilic-treated substrate surfaces was approximately 7° , indicating that the silanol groups were exposed due to their high wettability [2]. The composition ratio of nitrogen to carbon, oxygen, and silicon on the surface of each glass substrate was measured by XPS. The nitrogen composition was approximately 1% or less for the untreated and hydrophilic-treated substrates and 6.1% for the APS-treated substrate. The binding energy of the XPS spectrum was detected, confirming that nitrogen was derived from amino groups and indicating that the amino groups were introduced on the substrate by APS treatment. Therefore, the hydrophilic- and APS-treated substrate surfaces were negatively and positively charged, respectively [2].

Effect of liquid properties on the melting point of colloidal crystals

The relationship between the peak intensity and temperature of the measured reflectance spectra of colloidal crystals on the substrates is shown in Fig. 2. The peaks observed in the measurements were thought to originate from the body-centered cubic (bcc) densely packed surface. Using the particle diameter and volume fraction of the colloidal dispersion, it was possible to estimate the Bragg peak wavelength. From a 110-nm particle size and a 4.8-vol% volume fraction, the bcc peak wavelength was estimated to be 581 nm [14, 15]; however, the actual observed peak wavelength was approximately 625 nm. This discrepancy is attributable to inaccuracies in the particle size [2]. The point at which the peak of the reflection spectrum began to drop shows where the crystal structure began to collapse, indicating the crystal melting point. The colloidal crystal structure is formed by electrostatic interactions between the substrate and particles near the substrate surface and by interactions between particles within the crystal. When heat is applied to the structure, the particles undergo violent Brownian motion and the crystal melts.

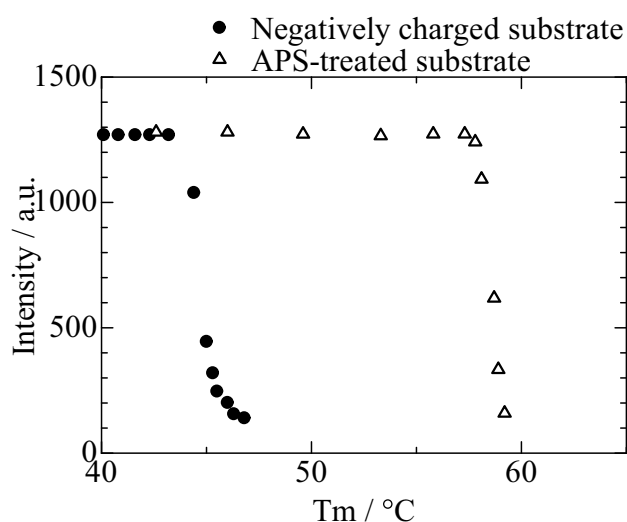


Fig. 2 Relative reflectance spectra of colloidal crystals (conductivity, 0.712 mS/m; pH, 4.598) on negatively charged and APS-treated substrates with increasing temperature

Figure 3 shows the melting points of colloidal crystals of various liquid properties plotted against pH for the measurements shown in Fig. 2. The pH values apply to the crystallization conditions of the colloidal crystals. We attempted to investigate the effect of ion concentrations and other factors, such as those in the electric double layer that vary with pH, on the melting point. For both treated substrates, the melting point change was bounded around pH 5.5. The melting points of the hydrophilic- and APS-treated substrates increased from approximately 40 to 60 °C and 80 °C, respectively, with decreasing pH from pH 5.5. Above pH 5.5, the melting points of both substrates changed from approximately 40 to 65 °C.

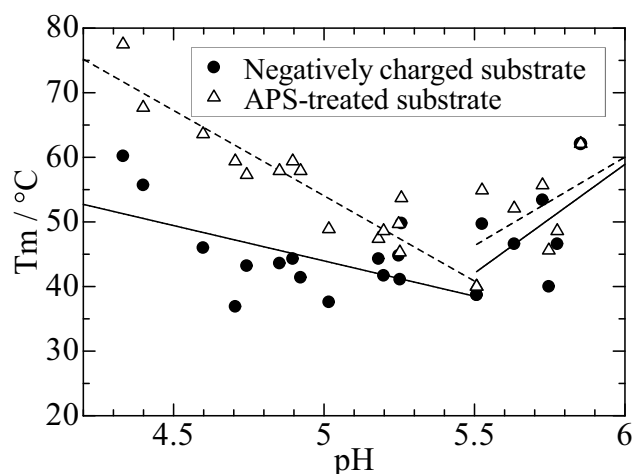


Fig. 3 Melting point plot of colloidal crystals formed on negatively charged and APS-treated substrates at various pH values

The melting point difference (APS – hydrophilic) was calculated from the results in Fig. 3 and plotted against pH in Fig. 4.

In Fig. 4, the melting point difference above pH 5.5 is approximately 0 °C, whereas the melting point difference below pH 5.5 varies from approximately 0 to 20 °C with decreasing pH.

Factors that contribute to an increase in the melting point of colloidal crystals are described. For the hydrophilic-treated substrate with silanol groups on the surface, electrostatic repulsion occurs between the colloidal particles and negatively charged substrate. The dissociation of the silanol groups is suppressed as the pH decreases. Therefore, the ion concentration in the electric double layer decreases and the repulsive force between the substrate and particles through the electric double layer decreases. In other words, the substrate's ability to bind the particles increases, and we believe that this enhances the thermal stabilizing effect of the crystals. It has been reported that the zeta potential ranges from approximately –60 to –40 mV for colloidal particles and from –75 to –50 mV for negatively charged substrates between pH 4 and 5.5 [16, 17]. Meanwhile, for the APS-treated substrate with amino groups on the surface, the amount of positive charge increases in the considered pH range because the dissociation of the basic amino groups is accelerated by a decrease in pH. It has also been reported that the zeta potential increases from approximately 45 to 70 mV between pH 4 and 5.5 [17]. Thus, the zeta potential of the APS-treated substrate, which has a positive charge opposite to that of the particles, tends to increase with decreasing pH, suggesting that the substrate binds the particles more easily and enhances the stabilizing effect. It is thought that the APS-treated substrate may increase the force required to bind the particles, thereby disorganizing the

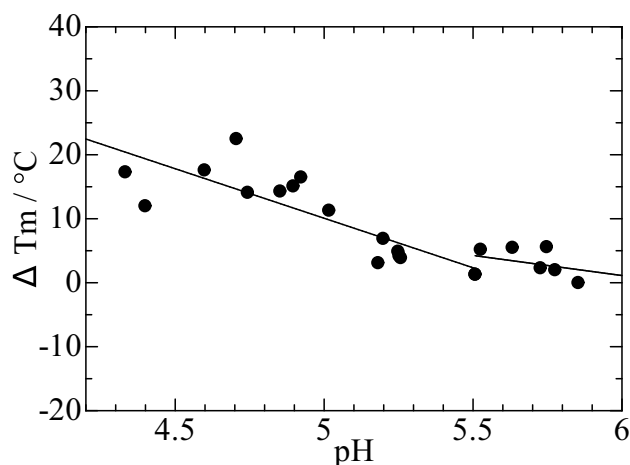


Fig. 4 Melting point difference (APS – hydrophilic) plots of colloidal crystals of various pH values

particle arrangement and preventing crystallization. However, the crystallization was confirmed. Next, above pH 5.5, the melting point increase rates of both substrates are similar, and the melting point difference is negligible. The zeta potential increases from approximately -60 to -70 mV for the colloidal particles with increasing pH and is nearly constant at approximately -75 and 50 mV for the hydrophilic- and APS-treated substrates, respectively. The change in zeta potential is confirmed only by the colloidal particles. The increase in the zeta potential of silica particles with increasing pH is due to the increase in the number of charges on the silica particles, suggesting that the electrostatic repulsive force through the electric double layer increases, thereby enhancing the stabilizing effect of the colloidal crystals. Therefore, it is thought that the particle-to-particle interactions exceeded the substrate-to-particle interactions and the substrate-to-particle interaction exceeded the particle-to-substrate interaction at pH 5.5 or lower. The pH 5.5 is seen as the inflection point of the graph showing the melting point of each substrate in Fig. 3. However, the reason for the inflection point at pH 5.5 is unclear. Therefore, in order to elucidate the reason for pH 5.5, it is necessary to find the relationship between the glass surface charge and particle surface charge as a function of the melting temperature and the pH of the colloidal crystal. To elucidate these effects, it is necessary to measure the zeta potentials of the glass substrate and the particle surface. We will continue to pay attention to this issue in our future research. The crystal melting may occur due to the increased Brownian motion of the particles as the temperature increased. However, at the present time, the completely melted colloidal crystals did not recrystallize when the temperature was lowered below the melting point. Therefore, the thermal reversibility of the colloidal crystals was irreversible. Convection due to the temperature gradient in the cell and dissolution due to increased ionic impurities produced from the cell as a mechanism for crystal melting could be the result of the increased ionic concentration. Furthermore, the APS on the substrate is easily hydrolyzed to form ionic amines. Crystal melting due to this is one possibility. A full comprehension of the working mechanism of the sandwich cell and a thorough elucidation of the phenomena inside the sandwich cell after crystals are melted deserve further research.

Patterning based on melting point difference

Figures 5 and 6 show colloidal crystals formed on a substrate with amino groups introduced by APS in the left half and on a negatively charged substrate in the right half, as confirmed by the melting points. As the temperature increases, the melting behavior of the colloidal dispersions is clearly observed. As shown in Figs. 3 and 4, colloidal crystals with low-pH values have large melting point differences, whereas

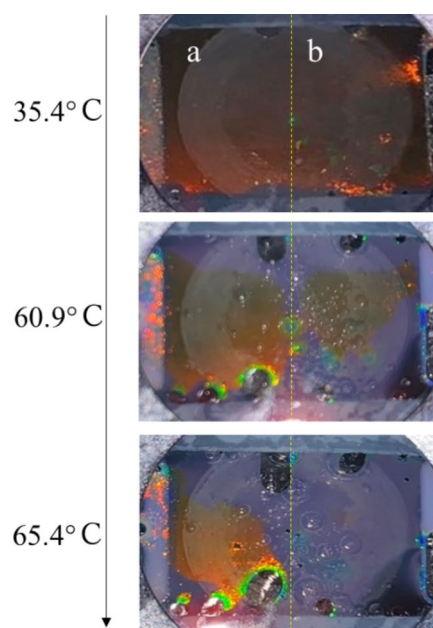


Fig. 5 Crystallization and melting behaviors of low-pH dispersions (conductivity, 0.575 mS/m; pH, 4.776) on **a** APS-treated substrate and **b** hydrophilic-treated substrate

those with pH values close to 5.5 have small melting point differences. In Fig. 5, only the low-pH colloidal crystals on the negatively charged substrate melted first at 60.9 °C, followed by those on the APS-treated substrate. Meanwhile, the high-pH colloidal crystal melting began almost simultaneously on both substrates (Fig. 6).

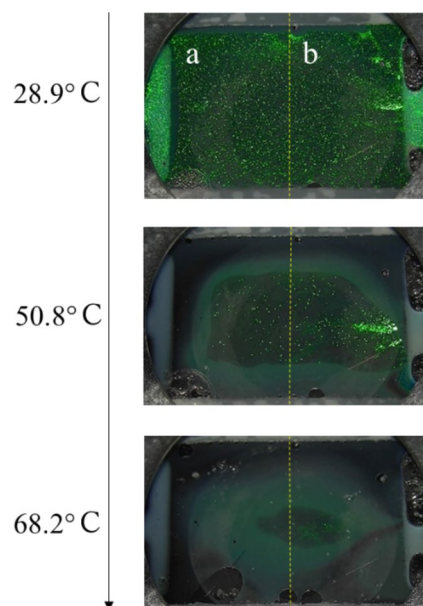


Fig. 6 Crystallization and melting behaviors of high pH dispersions (conductivity, 0.643 mS/m; pH, 5.853) on **a** APS-treated substrate and **b** hydrophilic-treated substrate

the article's Creative Commons licence and your intended use is not permitted by statutory regulation or exceeds the permitted use, you will need to obtain permission directly from the copyright holder. To view a copy of this licence, visit <http://creativecommons.org/licenses/by/4.0/>.

References

1. Xia Y, Gates B, Yin Y, Lu Y (2000) Monodispersed colloidal spheres: old materials with new applications. *Adv Mater* 12:693–713. [https://doi.org/10.1002/\(SICI\)1521-4095\(200005\)12:10%3c693::AID-ADMA693%3e3.0.CO;2-J](https://doi.org/10.1002/(SICI)1521-4095(200005)12:10%3c693::AID-ADMA693%3e3.0.CO;2-J)
2. Tsujino T, Tabata I, Hori T, Hirogaki K (2021) Influence of the surface charge of the substrate on the heat stability of electrostatic interactional colloidal crystals grown by heterogeneous nucleation. *Colloid Polym Sci* 299:1063–1069. <https://doi.org/10.1007/s00396-021-04828-3>
3. Yamanaka J, Murai M, Iwayama Y, Yonese M, Ito K, Sawada T (2004) One-directional crystal growth in charged colloidal silica dispersions driven by diffusion of base. *J Am Chem Soc* 126:7156–7157. <https://doi.org/10.1021/ja049164w>
4. Saboorian-Jooybari H, Chen Z (2019) Calculation of re-defined electrical double layer thickness in symmetrical electrolyte solutions. *Results Phys* 15:102501. <https://doi.org/10.1016/j.rinp.2019.102501>
5. Takeoka Y, Watanabe M (2003) Design of soft materials from colloidal crystals. *Sen'i Gakkaishi* 59:49–54. https://doi.org/10.2115/fiber.59.P_49
6. Okubo T (2008) Colloidal crystallization as compared with polymer crystallization. *Polym J* 40:882–890. <https://doi.org/10.1295/polymj.PJ2007182>
7. Kanai T, Sawada T, Maki I, Kitamura K (2003) Kossel line analysis of flow-aligned textures of colloidal crystals. *Jpn J Appl Phys* 42:L655–L657. <https://doi.org/10.1143/JJAP.42.L655>
8. Giersig M, Mulvaney P (1993) Preparation of ordered colloid monolayers by electrophoretic deposition. *Langmuir* 9:3408–3413. <https://doi.org/10.1021/la00036a014>
9. Liu Z, Zhang Q, Wang H, Li Y (2013) Structurally colored carbon fibers with controlled optical properties prepared by a fast and continuous electrophoretic deposition method. *Nanoscale* 5:6917–6922. <https://doi.org/10.1039/c3nr01766d>
10. Zhang X, Zhang J, Zhu D, Li X, Zhang X, Wang T, Yang B (2010) A universal approach to fabricate ordered colloidal crystals arrays based on electrostatic self-assembly. *Langmuir* 26:17936–17942. <https://doi.org/10.1021/la103778m>
11. Hirogaki K, Mizuno M, Kawasumi M, Tabata I, Hori T (2021) Prevention of lattice disproportionation of electrostatic interactional silica colloidal crystals grown via heterogeneous nucleation by cationic groups of substrate surfaces. *J Text Eng* 67:111–116. <https://doi.org/10.4188/jte.67.111>
12. Hirogaki K, Waki N, Tsujino T, Tabata I (2021) Influence of the cationic groups of substrate surfaces on the melting behavior of electrostatic interactional colloidal crystals grown via heterogeneous nucleation. *Colloid Polym Sci* 299:1399–1406. <https://doi.org/10.1007/s00396-021-04863-0>
13. Yoshida H, Yamanaka J, Koga T, Koga T, Ise N, Hashimoto T (1999) Transitions between ordered and disordered phases and their coexistence in dilute ionic colloidal dispersions. *Langmuir* 15:2684–2702. <https://doi.org/10.1021/la981316b>
14. Kakihara C, Toyotama A, Okuzono T, Yamanaka J, Ito K, Shinohara T, Tanigawa M, Sogami I (2015) Structural characterizations of charged colloidal crystals. *Int J Microgravity Sci Appl* 32:320205.1–320205.4
15. Tomita Y, Seki T, Fukaya N, Nishikawa S, Sato N, Imai M, Suko M, Takaki M, Aoyama Y, Toyotama A, Okuzono T (2018) Crystallization of charged colloids under microgravity during aircraft parabolic flights. *Int J Microgravity Sci Appl*. <https://doi.org/10.15011/jasma.35.3.350303>
16. Usui S, Sasaki H (1991) Dispersion and coagulation of fine particles-fundamentals and applications. *J Shigen Sozai* 107:585–591. <https://doi.org/10.2473/shigentosozai.107.585>
17. Yamada K, Yoshii S, Kumagai S, Fujiwara I, Nishio K, Okuda M, Matsukawa N, Yamashita I (2006) High-density and highly surface selective adsorption of protein–nanoparticle complexes by controlling electrostatic interaction. *Jpn J Appl Phys* 45:4259–4264. <https://doi.org/10.1143/JJAP.45.4259>

Publisher's Note Springer Nature remains neutral with regard to jurisdictional claims in published maps and institutional affiliations.